

Coalescence of polymeric sessile drops on an partially wettable substrate

Sarath Chandra Varma,¹ Aniruddha Saha,² and Alope Kumar^{1,*}

¹*Department of Mechanical Engineering, Indian Institute of Science, Bengaluru, India*

²*Department of Mechanical Engineering, Indian Institute of Technology Kharagpur, India*

Temporal dependence of height of the growing liquid bridge, for coalescing sessile polymeric fluid drops on a partially wettable substrate, is observed to follow a $t^{1/2}$ power-law behavior; in contrast, a $t^{2/3}$ growth has been reported for Newtonian fluids. The observed dynamics can be explained on the basis of a modified thin film equation under lubrication approximation using linear Phan-Thien-Tanner constitutive equation.

I. INTRODUCTION

The phenomenon of coalescence is of critical importance in various natural and industrial processes such as raindrop formation [1], atmospheric disturbances [2], coating and spraying [3, 4] and crystallisation [5]. In this singular event, the liquid topology changes rapidly to form a single daughter droplet. This singularity occurs during the formation of the meniscus connecting the two drops at the onset of coalescence. This merger of two sessile drops on a substrate has a rapid growth of the bridge initially, which later slows down in changing the shape of the merged droplet from oblong to roughly circular. In the case of coalescence in two hanging droplets the dynamics is universal in which surface tension, viscosity and inertial forces are important. However, such universality is not present in the coalescence of sessile drops due to the presence of substrate fluid interaction leading to significant viscous stresses causing the deviation from free drops coalescence. Such dependence on substrate leads to significant role of contact angle and spread length in governing the process.

Previous studies on sessile drop coalescence have focused on both highly viscous and apparently inviscid Newtonian fluids [6–9]. The temporal evolution of the bridge height h follows the scale of $t^{2/3}$, where t is time, for contact angles below 90° , contrasted by the $t^{1/2}$ for the contact angle of 90° [8, 10]. However, it is shown that the power law index α has a dependence on contact angle in which the bridge height scales as $h/R_o \sim (t/t_c)^\alpha$, where R_o is the half of the contact length, t_c is characteristic time given by $3\eta R_o/4\sigma \tan^4\theta$ for fluids with viscosity η , surface tension σ , making a contact angle of θ with the substrate [11]. α varied from 0.5 to 0.86 based on different fluids. Due to the presence of self similarity in the bridge connecting two drops a similarity solution was proposed for both symmetric and asymmetric coalescence of drops using the thin film equation [7].

Despite many applications of drop coalescence in rheologically complex fluids such as emulsions [12, 13], microfluidic applications [14] and interfacial rheology [15], the effect of presence of elasticity and characteristic time scale in the fluid has shown the deviation in the phenomenon compared to Newtonian fluids in the coalescence of free drops [16]. Unsurprisingly, the coalescence behaviour of such fluids on substrates has remained obscure.

*Electronic address: alokekumar@iisc.ac.in

In this letter we investigate the coalescence of two polymeric droplets on a substrate at early time instances. We show experimentally and theoretically, the time dependence of bridge height h_o between the two merging droplets each of viscosity η , contact angle θ , contact length $2R_o$, surface tension γ , and relaxation time λ due to the presence of elasticity owing to polymer chain relaxations. The experimental results are consistent with the modified thin film equation under lubrication approximation obtained from linear Phan-Thien-Tanner constitutive equation [17]. Similarity solution is not admissible to these fluids as compared to Newtonian fluids [7] due to the presence of inherent time scale of the fluid λ . Therefore, a numerical solution is obtained for the modified thin film equation. Initial shape of the droplets is obtained by employing the energy minimization technique by considering the droplets to be in thermodynamic equilibrium. Although many systems involve different polymers at different contact angles we used polyethylene oxide (PEO) to study the phenomenon as a representative fluid having a single contact angle.

II. MATERIALS AND METHOD

PEO solutions are prepared by adding appropriate quantity of PEO of molecular weight $M_w = 5000000\text{g/mol}$ obtained from Sigma Aldrich chemical co. in DI water to get various concentrations c of 0.1%, 0.2%, 0.3%, 0.4% and 0.5% w/v. All the solutions are stirred at 300 RPM for 24 hours. Concentrations of the PEO have been chosen such that the solutions are in semi-dilute unentangled and semi-dilute entangled regimes. The semi-dilute unentangled and entangled regimes are differentiated using entanglement concentration c_e . Entanglement concentration of PEO is $c_e \approx 6c^*$ [18] where, c^* is critical concentration[19]. c^* is obtained from the the intrinsic viscosity $[\eta]$ correlation $[\eta] = 0.072M_w^{0.65}$ [19].

Experiments were performed on a glass substrate. Preceding the experiments, the glass slides are cleansed with detergent and sonicated with acetone for 20 mins followed by sonication in water for 20 mins. Subsequently, the slides are dried in a hot air oven at 95°C for 30 mins.

Coalescence is achieved by creating two pendant drops of volume $\approx 11.5\mu\text{l}$ separated by a distance $l \approx 5.5\text{mm}$ each using syringe pumps. Substrate is brought towards the pendant drops with an approach velocity $\sim 10^{-4}$ m/s. Once the droplets touch the surface, they begin to spread and coalescence sets off instantaneously. The process is recorded using an Photron Fastcam mini high speed camera at 20000 FPS using Navitar lens. We perform further analysis of the images using custom algorithms in MATLAB.

Viscoelastic behaviour of the solutions is characterized by conducting rheology experiments on Anton Paar[®] MCR 302 rheometer using a cone and plate 40 mm, 1° geometry. Governing viscoelastic parameters such as shear viscosity η , and relaxation time λ are obtained by using the relations [20, 21]. Fig. 1(a) represents the rheological behaviour of PEO solutions where all the solutions have shown shear thinning behaviour [22]. Fig. 1(b) shows the variation in storage G' and loss modulus G'' with angular frequency ω for concentrations of 0.2% and 0.5% w/v. For concentrations c of 0.4% and 0.5% w/v, that are greater than entanglement concentration c_e , we observe comparable values of G' and G'' as shown in Fig. 1(b) for PEO 0.5% at lower time scales. In such time scales, concentrations in the range of $c^* < c < c_e$, which include 0.1%,0.2% and 0.3% yield distinct values of G' and G'' . Likewise, it is evident that elastic forces are equally important as the viscous forces in governing the phenomenon. Relaxation time λ is used to quantify the elastic behavior of the polymeric solutions. This intrinsic characteristic time scale λ associated with the polymer chains is estimated using the Zimm model [22]. The values of the relaxation time of the chosen solutions are

listed in Table 1.

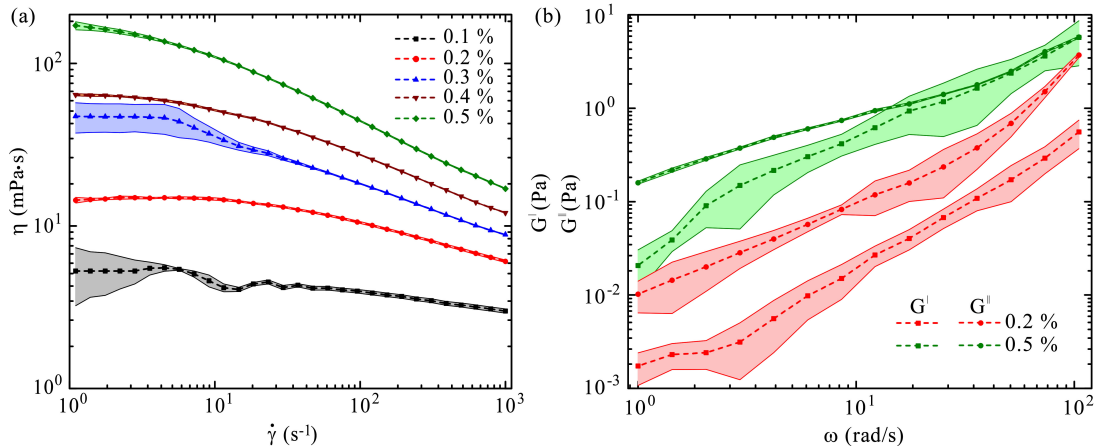


FIG. 1: (a) Variation of viscosity with shear rate for different concentrations of PEO. (b) Frequency sweep representing change in storage modulus G' and loss modulus G'' for 0.2% w/v and 0.5% w/v concentrations. (Standard deviation of the data has been represented through shades.)

TABLE 1: Rheological properties of the solutions

Concentration (w/v)	η_o (Pa.s)	λ (ms)
0.1%	0.006	4
0.2%	0.018	6
0.3%	0.0458	8
0.4%	0.06	74
0.5%	0.2	115

III. RESULTS AND DISCUSSION

Capillarity initiates the coalescence in sessile drops immediately after the drops come into contact, the phenomenon proceeds via the formation of a liquid bridge of a instantaneous height $h_0(t)$ as depicted in Fig. 2(a). The kinematics of such a formation is further guided by the local curvature effects and surface tension γ . Such evolution of the liquid bridge during coalescence of an aqueous solution of 0.5% w/v PEO and DI water at different time instants are shown in Fig. 2(b) and (c) respectively. The geometry is associated with a contact length of $2R_0 \approx 5.25 \pm 0.25$ mm and an interfacial contact angle of $\theta \approx 35 \pm 3^\circ$ for all the polymer solutions and DI water.

Temporal variation of bridge height h_0 for the polymer solution has followed the power law variation as shown in Fig. 3. The linear part which is shown as the region of interest in Fig. 3 is considered for analysis. The power law index of this linear regime for polymer solutions is 0.5 ± 0.025 which can be contrasted with the exponent exhibited in Newtonian fluids [7, 8, 10]. As the droplets touch the substrate, the polymer chain tries to elongate along the shear direction. In the initial instances, when the drops begin to merge the polymer chains are highly elongated, which tries to inhibit the coalescence, leading to deviation of exponent from Newtonian behaviour. Using a scaling analysis,

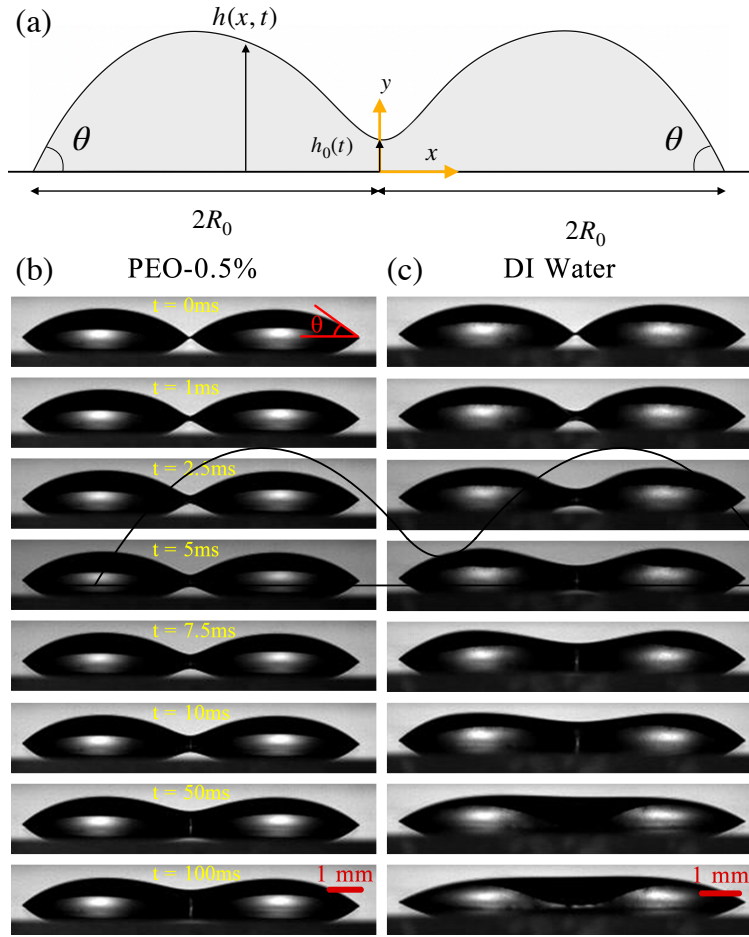


FIG. 2: (a) Schematic of neck region during coalescence, (b) neck radius evolution of 0.5% w/v concentration of PEO on the left compared with (c) DI water on the right at different instants.

the polymer chain elongations characterised by elastic forces is represented using Weissenberg number $Wi = \lambda u_c / l_c$, where u_c and l_c represent characteristic velocity and length scales respectively. The characteristic scales associated with the flow are $u_c \sim \langle \partial h / \partial t \rangle$ and $l_c \sim R_0 \tan \theta$. It is observed that $Wi \sim \mathcal{O}(1)$ and $Wi \sim \mathcal{O}(0.1)$ for higher and lower concentrations respectively, which agrees with Fig. 1(b). This explains the increased dominance of elastic forces with higher polymeric concentrations. However, the power law index for the solutions of $Wi \sim \mathcal{O}(1)$ and $Wi \sim \mathcal{O}(0.1)$ remained constant as 0.5 due to the same shear rate during the process.

The governing equation for thin films for physically unsteady flows pertains to the solution of the Stokes equation in the lubrication limit with density ρ and viscosity η . In this limit, the momentum equation in the x -direction thus becomes: $0 = -\nabla_x P + (\nabla \cdot \boldsymbol{\tau})_x$, where the velocity field is $\mathbf{v} = \mathbf{v}(u, v, 0)$, and the extra stress of the fluid and the hydrostatic pressure are represented by $\boldsymbol{\tau}$ and P respectively. The stress tensor $\boldsymbol{\tau}$ satisfies the linear PTT constitutive relation $\boldsymbol{\tau} f(\tau) + \lambda \overset{\nabla}{\boldsymbol{\tau}} = 2\eta \mathbf{D}$, where $f(\tau) = 1 + \frac{k\lambda}{\eta} Tr(\boldsymbol{\tau})$. We get the velocity profile as

$$u = \frac{1}{2\eta} \frac{dP}{dx} \left[y^2 - 2yh + \frac{2k\lambda^2}{\eta^2} \left(\frac{dP}{dx} \right)^2 \left(3y^2h^2 - 2yh^3 - 2hy^3 + \frac{y^4}{2} \right) \right] \quad (1)$$

The integral form of the thin film equation obtained from lubrication theory is written as: $\frac{\partial h}{\partial t} + u \frac{\partial h}{\partial x} = - \int_0^h \frac{\partial u}{\partial x} dy$, and the pressure gradient is written in terms of hydrostatic and surface curvature Γ for a surface tension γ as $\rho g \frac{\partial h}{\partial x} - \gamma \frac{\partial \Gamma}{\partial x}$,

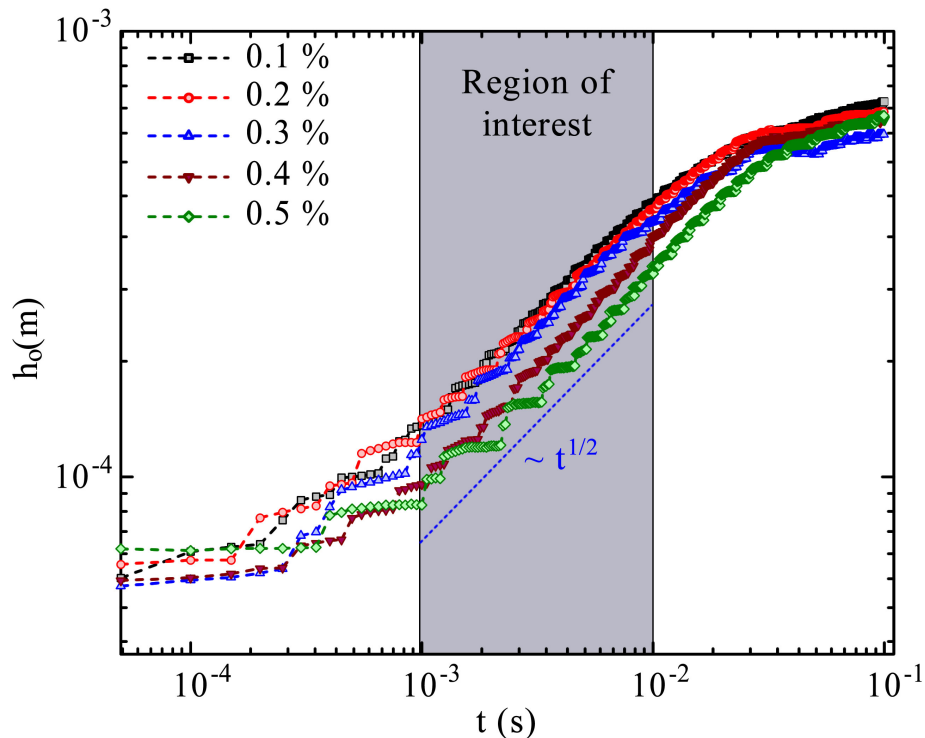


FIG. 3: Temporal evolution of bridge height for various concentrations of PEO solutions along with DI water as control case.

which led to the thin-film equation as:

$$\frac{\partial h}{\partial t} + \frac{\gamma}{3\eta} \frac{\partial}{\partial x} \left[h^3 \frac{\partial^3 h}{\partial x^3} + \frac{6k\lambda^2\gamma^2}{5\eta^2} h^5 \left(\frac{\partial^3 h}{\partial x^3} \right)^3 \right] = 0 \quad (2)$$

Droplet shape $h(x, t)$ is symmetrical about the contact bridge that connects the two sessile drops. The sessile drop prior to coalescence is considered to be in thermodynamic equilibrium and occupies minimal free energy, that gives its free shape. Using the Young-Dupré equation contact angle is written as θ as $\cos\theta = (\gamma_{sg} - \gamma_{sl})/\gamma_{lg}$, where γ_{sg} , γ_{sl} and γ_{lg} are the surface tension values of the solid-gas, the liquid-solid, and the liquid-gas surface, respectively. We represent the droplet shape in (R, ψ) coordinates where the origin coincides with the midpoint of the contact line, and ψ is taken clockwise. The thermodynamic potential [23] is contributed by the bulk, the interfaces and gravitational potential energy: $G = (\gamma + \lambda_l) (\pi R/\sqrt{2})^2 + \pi \int_0^{\pi/2} [2\gamma R\sqrt{\dot{R}^2 + R^2} + \frac{\rho}{2}gR^4 \cos\psi] \sin\psi d\psi$, where $\gamma = \gamma_{lg}$, λ_l is the partial free energy of the liquid-solid bonding, per unit area of their contact interface [24]. We take the volume of the drop as the constraint $V = 2\pi/3 \int_0^{\pi/2} R^3 \sin\psi d\psi$ and perform minimisation of the expression $G/\gamma - \nu V$, where ν is the Lagrange multiplier. We apply Euler-Lagrange minimisation criterion to yield:

$$\left[\frac{2\dot{R}^2 + R^2 - \ddot{R}R}{(\dot{R}^2 + R^2)^{3/2}} + \frac{R - \dot{R} \cot\psi}{R\sqrt{\dot{R}^2 + R^2}} \right] + \frac{\rho g}{\gamma} R \cos\psi = \nu \quad (3)$$

with the boundary conditions: $\dot{R}(0) = \cos\psi \sqrt{R(0)^2 + \dot{R}(0)^2}$ and $\dot{R}(\pi/2) = 0$. Eq. (3) has been solved using shooting method with 4th order Runge-Kutta formulation. The initial shape $h(x, 0)$ thus becomes $R(\psi)$, where $R\cos\psi = x$. For modelling of the coalescence, the conjunction of two adjacent shapes $h(x, 0)$ is considered and the coalescence proceeds with $h(0, t \rightarrow 0^+) = h_y$, where h_y is a sufficient small value denoting initial drop contact. The evolution

of the drop starts with the initial condition, and the evolution obeys symmetric boundary conditions $h'(0,t) = 0$, $h(2R_0,t) = 0$ and conservation of mass $h'''(0,t) = 0$. The contact angle remains unchanged throughout such that $h'(2R_0,t) = -\tan\alpha$. Explicit time-marching schemes have been used considering time steps that maintain numerical stability to obtain solution of Eq. (2). We non-dimensionalise h_0 by l_c and time t by λ as represented by Fig. 4(a). Fig. 4(a) demonstrates the agreement between the experimental and the computational results, where h_0 and t have

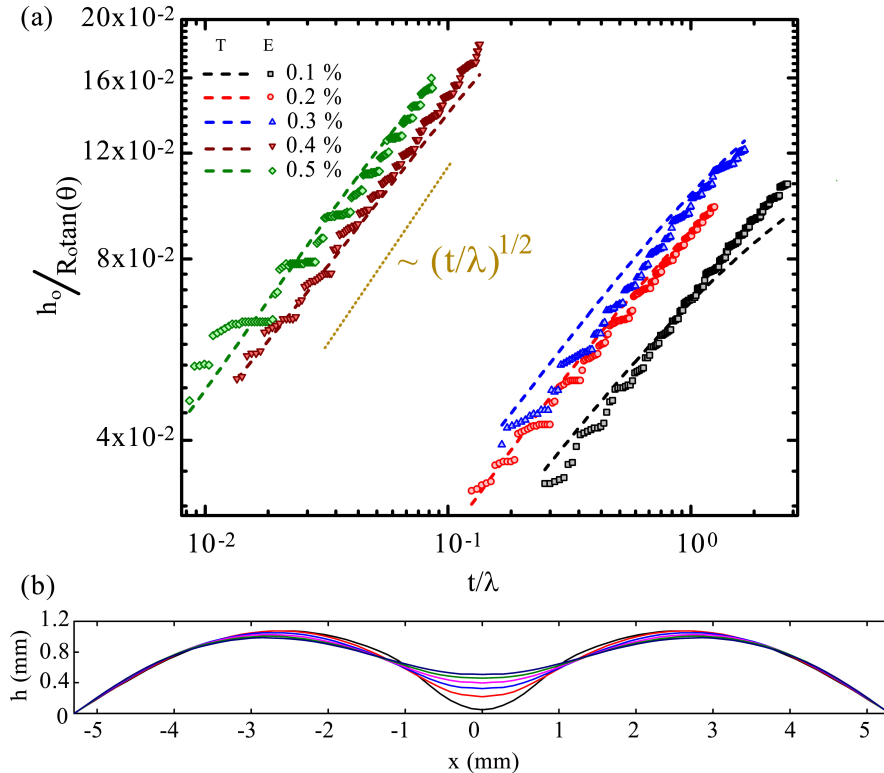


FIG. 4: (a) Comparison of non-dimensional bridge height evolution between experiments and numerical solution of Eq. (2) for 0.2% w/v and 0.4% w/v concentrations. (b) Drop shape during the coalescence process from 0s to 10ms with an increment of 2ms for 0.5% w/v. (Note:T represents theoretical, E represents experimental)

been non-dimensionalised with l_c and λ respectively. The temporal evolution of the droplet shape has been captured in Fig. 4(b) for 0.5% w/v concentration and are in good agreement with the experiments as in Fig. 2(b). The additional term in Eq. (2) representing the elasticity of the fluid led to the deviation of the bridge growth from Newtonian fluids.

IV. CONCLUSION

The current dynamical map presented for sessile drop coalescence involving polymeric fluids extends opens up a newer perspective in terms of analysis methods and complexity of the physics. We have been able to capture the accurate description of of the coalescence through a modified thin-film equation that can be extended for a wider class of non-Newtonian fluids. The present study has been carried out over a concentration regime of semi-dilute unentangled and semi-dilute entangled that have shown identical temporal variation as well. We have performed the analysis in the frontal plane and the temporal variation of horizontal bridge growth can be extended from this study.

In this time domain, the process has been observed to progress following a contact angle and contact line. The fluid-substrate interaction holds key insights to the pinning of drop during the process. The surrounding fluid effect can be an important factor behind the dynamics, which has been neglected by using air. This requires further exploration on the domain of its applicability which might culminate into the explanation of a merger phenomenon between two fluid ensembles with characteristic scales ranging quite high above the values which have been incorporated in this experiment. Future work should be dedicated to a variety of cases, such as with bio-fluids, colloids and in an attempt to unify the physics of this evolutionary phenomena.

-
- [1] E. Villermaux and B. Bossa, *Nature Physics* **5**, 697 (2009).
 - [2] P. L. Smith, D. J. Musil, A. G. Detwiler, and R. Ramachandran, *Journal of Applied Meteorology* **38**, 145 (1999).
 - [3] N. Ashgriz and J. Poo, *Journal of Fluid Mechanics* **221**, 183 (1990).
 - [4] H. Djohari, J. I. Martínez-Herrera, and J. J. Derby, *Chemical Engineering Science* **64**, 3799 (2009).
 - [5] C. Klopp, T. Trittel, and R. Stannarius, *Soft Matter* **16**, 4607 (2020).
 - [6] W. D. Ristenpart, P. M. McCalla, R. V. Roy, and H. A. Stone, *Phys. Rev. Lett.* **97**, 064501 (2006).
 - [7] J. F. Hernández-Sánchez, L. A. Lubbers, A. Eddi, and J. H. Snoeijer, *Phys. Rev. Lett.* **109**, 184502 (2012).
 - [8] A. Eddi, K. G. Winkels, and J. H. Snoeijer, *Phys. Rev. Lett.* **111**, 144502 (2013).
 - [9] N. Kapur and P. H. Gaskell, *Phys. Rev. E* **75**, 056315 (2007).
 - [10] Y. Sui, M. Maglio, P. D. M. Spelt, D. Legendre, and H. Ding, *Physics of Fluids* **25**, 101701 (2013).
 - [11] M. W. Lee, D. K. Kang, S. S. Yoon, and A. L. Yarin, *Langmuir* **28**, 3791 (2012).
 - [12] A. B. Pawar, M. Caggioni, R. Ergun, R. W. Hartel, and P. T. Spicer, *Soft Matter* **7**, 7710 (2011).
 - [13] C. P. Whitby and M. Krebsz, *Soft Matter* **10**, 4848 (2014).
 - [14] T. Krebs, K. Schroën, and R. Boom, *Soft Matter* **8**, 10650 (2012).
 - [15] S. Vandebril, J. Vermant, and P. Moldenaers, *Soft Matter* **6**, 3353 (2010).
 - [16] S. C. Varma, A. Saha, S. Mukherjee, A. Bandopadhyay, A. Kumar, and S. Chakraborty, *Soft Matter* (2020).
 - [17] R. I. Tanner and S. Nasser, *Journal of Non-Newtonian Fluid Mechanics* **116**, 1 (2003).
 - [18] O. Arnolds, H. Buggisch, D. Sachsenheimer, and N. Willenbacher, *Rheologica Acta* **49**, 1207 (2010).
 - [19] V. Tirtaatmadja, G. H. McKinley, and J. J. Cooper-White, *Physics of Fluids* **18**, 043101 (2006).
 - [20] Y. Liu, Y. Jun, and V. Steinberg, *Journal of Rheology* **53**, 1069 (2009).
 - [21] F. Del Giudice, G. D'Avino, F. Greco, I. De Santo, P. A. Netti, and P. L. Maffettone, *Lab on a Chip* **15**, 783 (2015).
 - [22] R. B. Bird, R. C. Armstrong, and O. Hassager, *Dynamics of polymeric liquids. Vol. 1, 2nd Ed. : Fluid mechanics* (Wiley, 1987).
 - [23] J. W. Bullard and J. W. Bullard, *Thermodynamics of Sessile Drops on a Rigid Substrate: A Comparison of Two Theories* (US Department of Commerce, National Institute of Standards and Technology, 2005).
 - [24] A. W. Searcy, *Scripta materialia* **40** (1999).